Dual-porosity and kinematic wave approaches to assess the degree of preferential flow in an unsaturated soil

ABDALLAH ALAOUI, PETER GERMANN
Soil Science Section, Department of Geography, University of Bern, Hallerstrasse 12, CH-3012 Bern, Switzerland
germann@giub.unibe.ch

NICHOLAS JARVIS
Department of Soil Sciences, Swedish University of Agricultural Sciences, Box 7014, S-75007 Uppsala, Sweden

MARCO ACUTIS
Department of Agricultural Engineering and Agronomy, University of Naples Federico II, I-80125 Naples, Italy

Abstract The purpose of this study was to assess the degree of preferential flow in an unsaturated soil column using two different models: the dual-porosity model, MACRO, and the kinematic wave approach (KWA) based on boundary-layer flow theory. The soil column experiments consisted of six infiltrations with intensities varying from 15 to 101 mm h^{-1}. Bromide solution was also infiltrated at an intensity of 79 mm h^{-1} and a concentration of 80 mg l^{-1}. Both MACRO and the KWA indicated the absence of pure preferential flow. The KWA indicated intermediate flow with dispersion of the wetting front with depth, whereas MACRO indicated flow dominated by the diffusion of capillary potential. These results shed light on the transition between flows dominated by momentum dissipation and by diffusion of capillary potential. The absence of pure macropore flow in the structured sandy soil is mainly due to efficient lateral mass exchange in this material.

Key words macropore flow; dual-porosity model; kinematic wave approach; unsaturated soil

Modèle à double porosité et théorie de l'onde cinématique pour déterminer l'importance de l'écoulement préférentiel dans un sol non saturé

Résumé Le but de cette étude est de déterminer l'importance de l'écoulement préférentiel dans une colonne de sol non saturé en utilisant deux modèles différents: le modèle à double porosité MACRO et l'approche par onde cinématique (AOC) basée sur la théorie de la couche limite du flux. Les expériences conduites sur le sol ont consisté en six irrigations d'intensité variant de 15 à 101 mm h^{-1}. Une solution de bromures a été infiltrée avec une intensité de 79 mm h^{-1} et une concentration de 80 mg l^{-1}. Les deux approches ont montré l'absence de flux préférentiel pur. L'AOC a mis en évidence un flux intermédiaire avec une dispersion du front d'humectation en profondeur, tandis que le modèle MACRO a présenté un flux diffusif. Les deux approches ont mis en évidence la transition entre un flux dominé par la dissipation de l'énergie cinétique et la diffusion du potentiel capillaire. L'absence de flux préférentiel dans ce sol sableux structuré est due à un important échange latéral de masse.

Mots clefs écoulement dans les macropores; modèle à double porosité; approche par onde cinématique; sol non saturé

INTRODUCTION

Flow and transport in structured porous media are frequently described using double- (or dual) porosity models. Such approaches assume that the medium consists of two

regions, one associated with the macropore or fracture network and the other with a less permeable pore system of soil aggregates or rock matrix blocks. Typically, dissipation of momentum dominates flow in well structured soils at high moisture contents and at high infiltration rates, whereas diffusion of capillary potential dominates flow in homogeneous soils over a broader range of moisture contents and at low infiltration rates.

Approaches to flow in structured soils can be divided in two major groups:

(a) Approaches based on Richards' (1931) equation for water flow in the matrix domain (i.e. diffusion of potential energy) in combination with other approximations for macropore flow. The two domains are considered separately from one another with some account for interactions.

(b) The kinematic wave theory (Lighthill & Whitham, 1955) based on the dissipation of momentum was proposed by Beven & Germann (1981) and further developed by Germann (1985, 1990). A power function relates the water flux to the mobile volumetric water content.

As an example of the first type of approach, Hoogmoed & Bouma (1980) proposed a two-domain model to simulate flow in clay soils, assuming that the matrix and the macropores comprise separate domains for vertical flows with lateral exchanges of water and solutes. Chen & Wagenet (1992) simulated water and chemical transport by combining the Richards (1931) equation for transport in the soil domain with the Hagen-Poiseuille and Chezy-Manning equations for macropore transport. Jarvis (1994) developed a physically-based model (MACRO) of water and solute transport in macroporous soil. The model divides the total soil porosity into macropores and micropores. Water flow in micropores is calculated with the Richards equation, while macropore flow is simulated as a power law function of the saturation level in macropores. This may be considered as a numerical approximation to the analytical kinematic wave equation (Germann, 1985). An effective diffusion path length d, controls mass exchange between the domains. Net rainfall is partitioned into an amount taken up by micropores and an excess amount of water flowing into macropores under non-equilibrium conditions bypassing the matrix flow.

In the second type of approach, Germann & Di Pietro (1999) used analytical kinematic wave theory to describe macropore flow. They suggest that water in larger continuous pores may advance during infiltration so fast that it overshoots local capillary potential. Flow in films and rivulets is dominated by momentum dissipation due to viscosity and is dealt with by the theory of laminar boundary-layer flow. The theory is based on Newton's law of shear which Germann (1990), among others, applied to flow in structured and unsaturated soils.

The objectives of this study were:

1. To assess whether the type of water flow mechanism (i.e. whether water flows predominantly through the matrix or as non-equilibrium macropore flow) could be distinguished using two different approaches: (a) the dual-porosity/dual-permeability model, MACRO; and (b) the kinematic wave approach, KWA, based on boundary-layer flow theory.
2. To check if the derived parameter values, especially those characterizing the flow type, in the two models are comparable.

MATERIAL AND METHODS

The soil used in this study originates from calcareous silty-sandy lake sediments from the St Peter's Island in Lake Bienne (Switzerland). The island formed during the last 120 years after the lake level had been lowered by several metres. The horizon 0–0.16 m is well structured with a porosity of 0.52 m^3 m^{-3}. The porosity is 0.50 m^3 m^{-3} in the lower part of the profile below 0.16 m, while the pH is 7 throughout. The bulk density increases slightly from 1.07 to 1.16 mg m^{-3} from the topsoil to the subsoil. The texture is sandy loam in the topsoil between 0 and 0.16 m, loamy sand between 0.16 and 0.27 m and sand in the subsoil below 0.27 m. The soil is a fluvisol characterized by a well-aggregated A_h horizon (0–0.05 m), a B horizon at 0.15–0.45 m depth, and a C horizon below 0.45 m. The vegetation consists of herbs and grasses. A network of macropores comprising root and earthworm channels was visible to 0.70–0.80 m depth.

A column of undisturbed soil 0.39 m in diameter and 0.43 m in height was prepared by vertically driving a bevelled stainless steel cylinder into the ground while continuously removing the surrounding soil material (Mdaghri-Alaoui, 1998).

Saturated hydraulic conductivity was determined on samples of undisturbed soil with a diameter of 55 mm and length of 42 mm, taken at 50-mm depth increments throughout the soil profile. Saturated hydraulic conductivity was determined with a constant head permeameter (Klute & Dirksen, 1986).

Irrigation was supplied by a rainfall simulator consisting of a metallic disc perforated with 72 holes connected by small tubes to a reservoir. A motor rotated the metallic disc and a pump controlled irrigation intensity and duration. Soil water contents at depths of 0.12, 0.26 and 0.33 m were measured with time domain reflectrometry (TDR, Tektronix 1502B cable tester), with 0.30-m wave guides (two parallel rods of 6 mm diameter and 35 mm apart) inserted horizontally into the column. Calibration was performed according to Roth *et al*. (1990) who separated the impact of the wave-guide geometry from the soil properties, such as bulk density and the content of clay and organic matter, on the dielectric number. The limit of significant differences among individual measurements with the same wave-guide was assessed at utmost 0.002 m^3 m^{-3}. Matric potential was measured with three tensiometers at depths of 0.12, 0.26 and 0.40 m. The tensiometer cups were 50 mm long with a diameter of 6 mm. To support the column, a disc with square holes was placed at the bottom.

The soil column was placed on a funnel connected to an outflow collector equipped with a pressure transducer. A data-logger measured automatically water content, matric potential and drainage flow. Six successive infiltrations of increasing intensity were applied to the soil column (Table 1). Steady-state conditions were established for each irrigation. Time domain reflectrometry measurements were made every 300 s. No application exceeded the soil infiltration rate as no ponding was observed. In all six cases, initial breakthrough occurred in the centre of the bottom of the soil column and not at the periphery.

A total of 9.6 l of a KBr solution with a concentration of 80 mg l^{-1} Br^- was applied to the soil surface during 3570 seconds using the rainfall simulator. The intensity was 79 mm h^{-1} (2.2×10^{-5} m s^{-1}). Bromide concentrations were measured with a Br^- ion selective electrode (Metrohom, no. 6.0502.100) having a double junction reference electrode. Ionic strength adjuster 25 ml of KNO_3 was added to every 25 ml sample. The error of the measurements was less than 2%.

Table 1 Characteristics of infiltration experiments conducted on St Peter's Island soil.

Run	Intensity ($mm\ h^{-1}$)	Duration (h)	Initial water content ($m^3\ m^{-3}$): 0.12 m	0.26 m	0.33 m	Max. water content ($m^3\ m^{-3}$): 0.12 m	0.26 m	0.33 m
1	14.8	3.86	0.382	0.34	0.357	0.46	0.39	0.437
2	38.2	2.78	0.376	0.321	0.339	0.489	0.416	0.456
3	79.2	1.14	0.38	0.368	0.366	0.50	0.50	0.494
4	82.8	1.24	0.367	0.277	0.322	0.50	0.50	0.493
5	94.3	1.11	0.386	0.292	0.31	0.514	0.50	0.49
6	100.8	0.83	0.367	0.333	0.333	0.52	0.50	0.50

THEORY

MACRO model

The MACRO model is a mechanistic dual-porosity model applicable to water movement and solute transport in soils. The model is briefly introduced here. For more details, see Jarvis (1994).

The total porosity is partitioned at a boundary water content/potential into macropores and micropores. Each domain is characterized by a degree of saturation, a conductivity and a flux, while interaction terms account for convective and diffusive exchange between flow domains. Water movement in the micropores is calculated with the Richards equation including a sink term to account for root water uptake. The soil hydraulic properties in the micropores are described by the functions of Brooks & Corey (1964) and Mualem (1976):

$$\psi_{mi} = \psi_b S_{mi}^{-1/\lambda} \tag{1}$$

$$K_{mi} = K_b S_{mi}^{n+2+2/\lambda} \tag{2}$$

$$S_{mi} = \frac{\theta_{mi} - \theta_r}{\theta_b - \theta_r} \tag{3}$$

where the subscript *mi* refers to micropores; θ_b ($m^3\ m^{-3}$), ψ_b (m) and K_b ($m\ s^{-1}$) are the water content, pressure head and hydraulic conductivity at the boundary between micro- and macropores, respectively; θ is the current water content; λ (-) is the pore size distribution index; θ_r ($m^3\ m^{-3}$) is the residual water content; S ($m^3\ m^{-3}$) is the degree of saturation; and n (-) is the tortuosity factor.

Water flow in the macropores is calculated with an approach derived from Darcy's law assuming a unit hydraulic gradient and simple power law function to represent the unsaturated hydraulic conductivity:

$$q_{ma} = (K_s - K_b)\left(\frac{\theta_{ma}}{\theta_s - \theta_b}\right)^{n^*} \tag{4}$$

where the subscript *ma* refers to macropores; θ_{ma} ($m^3\ m^{-3}$) is the macropore water content; θ_s ($m^3\ m^{-3}$) is the saturated water content; K_s ($m\ s^{-1}$) is the saturated hydraulic conductivity; and n^* (-) reflects pore size distribution and tortuosity in the macropore system. Solute transport in the micropore domain is predicted using the convection–dispersion equation, written here for a non-reactive solute:

$$\frac{\partial(\theta C)}{\partial t} = \frac{\partial}{\partial z}\left(D\theta \frac{\partial C}{\partial z} - qC \right) + T_s \tag{5}$$

where C (kg m^{-3}) is the solute concentration; q (m s^{-1}) is the water flow rate; T_s (s^{-1}) is a source/sink term for exchange of solute with the macropore domain; z (m) is the depth; t (s) is the time; and D (m^2 s^{-1}) is the dispersion coefficient given by:

$$D = D_v v + D_0 f \tag{6}$$

where D_0 (m^2 s^{-1}) is the diffusion coefficient of the solute in free water; f (-) is the impedance factor; D_v (m) is the dispersivity; and v (m s^{-1}) is the pore water velocity in micropores given by q_{mi}/θ_{mi}. Solute transport is treated in the same way in micropores and macropores, except that dispersion is neglected in the macropores where convection is assumed to dominate.

The surface boundary condition in the MACRO model partitions the net rainfall into an amount taken up by micropores and an excess amount of water flowing into macropores. This partitioning is determined by a simple description of the infiltration capacity of the micropores. Various alternative options for the bottom boundary condition are available in the model (i.e. constant hydraulic gradient, zero flux, constant potential with or without inflow of water at the bottom boundary, or lysimeter with free drainage).

Mass transfer is calculated using a physically-based expression (Jarvis, 1994) derived from exact diffusion models by a first-order approximation. The source/sink term, T_s, for mass transfer of solute is given by a combination of a diffusion component (van Genuchten & Dalton, 1986; Valocchi, 1990) and a mass flow component:

$$T_s = \left(\frac{3 D_a \theta_{mi}}{d^2} \right)\left(C_{ma} - C_{mi} \right) + S_w C' \tag{7}$$

where d is an effective diffusion path length; the subscripts *ma* and *mi* refer to macropores and micropores, respectively; the prime notation indicates either macro- or micropores depending upon the direction of water flow (S_w); and D_a is an effective diffusion coefficient given by:

$$D_a = D_0 f S_{ma} \tag{8}$$

where S_{ma} is the degree of saturation in the macropores, introduced to account for incomplete wetted contact area between the domains. The rate of lateral water exchange from macropores to micropores is also treated as a first-order approximation to a diffusion-type process (Booltink *et al*., 1993). Assuming that gravity has negligible influence, S_w is given by:

$$S_w = \left[\frac{3 D_w \gamma_w}{d^2} \right]\left(\theta_b - \theta \right) \tag{9}$$

where D_w (m^2 s^{-1}) is an effective diffusivity and γ_w (-) is a scaling factor (Jarvis, 1994). The effective water diffusivity is assumed to be given by:

$$D_w = \left(\frac{D_{\theta b} + D_{\theta mi}}{2} \right) S_{ma} \tag{10}$$

where $D_{\theta b}$ and $D_{\theta mi}$ are the water diffusivities at the boundary water content and the

current micropore water content, respectively. Using the Mualem/Brooks-Corey model for soil hydraulic properties, $D_{\theta mi}$ is given by:

$$D_{\theta mi} = \frac{K_b \psi_b S_{mi}^{n+1/\lambda+1}}{\lambda(\theta_b - \theta_r)} \tag{11}$$

while $D_{\theta b}$ is given by setting S_{mi} in equation (11) to unity.

If the micropores become oversaturated (i.e. $\theta_{mi} > \theta_b$), then the excess water is routed instantaneously into the macropores and the second term on the right-hand side of equation (7) is adjusted accordingly.

Kinematic wave approach (KWA)

The theory of laminar boundary-layer flow deals explicitly with momentum dissipation due to viscosity, and the theory of kinematic waves provides the mathematical tool to apply it to flow in soils. Accordingly, the wetting and draining fronts of an input pulse constitute moving shock boundaries which are dealt with using the method of characteristics (Germann & Di Pietro, 1996).

Soil moisture contributing to the total flow and the fraction contributing to rapid flow are abbreviated by θ and w (both in $m^3\ m^{-3}$), respectively ($w < \theta$) (see Fig. 1).

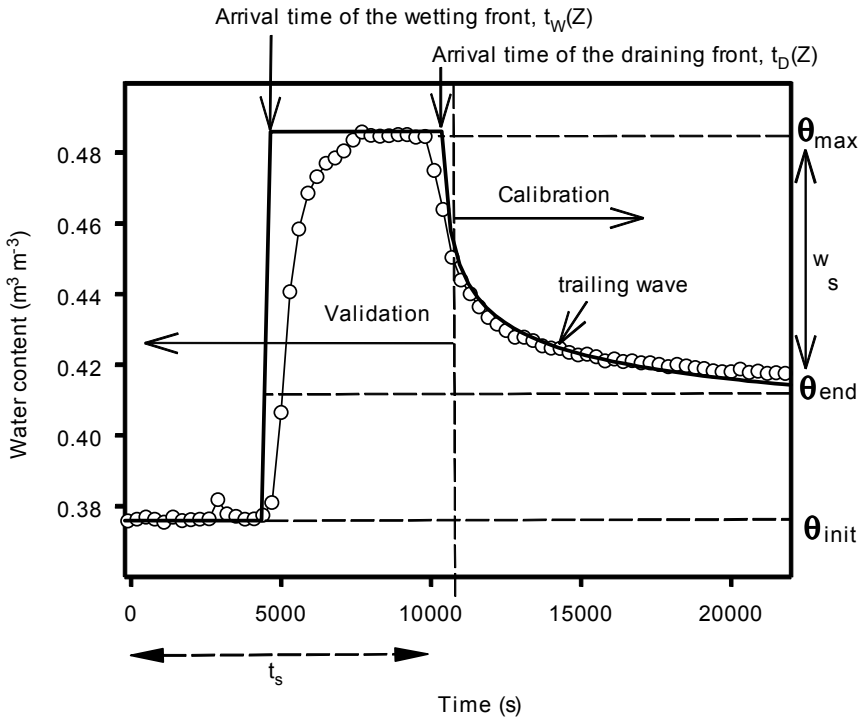

Fig. 1 Evolution of soil moisture and definition of the parameters of the kinematic wave approach [t_s is the duration on infiltration; t_W is the arrival time of wetting front; t_D is the arrival time of draining front; $\theta(Z,t)$ is the total soil moisture measured at depth Z and time t; θ_{init} is the soil moisture prior to infiltration; θ_{end} is the final water content following the passage of the kinematic wave; and $w(Z,t)$ is the fraction of soil moisture contributing to rapid flow ($w(Z,t) = \theta(Z,t) - \theta_{end}$)].

Beven & Germann (1981) first proposed a relationship between the macropore volumetric flux, q, and macropore water content, w, of the following form:

$$q = bw^a \tag{12}$$

where b (m s^{-1}) is conductance and a is a dimensionless exponent. The continuity equation of a kinematic wave is:

$$\frac{\partial q}{\partial t} + c\,\frac{\partial q}{\partial z} = 0 \tag{13}$$

where the celerity c (m s^{-1}), which represents the propagation velocity of changes of mobile soil moisture, is defined as:

$$c = \frac{\mathrm{d}q}{\mathrm{d}w} = ab^{1/a}q^{(a-1)/a} = abw^{a-1} = \left.\frac{\mathrm{d}z}{\mathrm{d}t}\right|_{q,w} \tag{14}$$

The celerity of the wetting shock front is:

$$c_W = \frac{q}{w} = b^{1/a}q^{(a-1)/a} = bw^{a-1} = \left.\frac{\mathrm{d}z}{\mathrm{d}t}\right|_{q,w} \tag{15}$$

The water input to the soil surface is considered as a rectangular pulse of volume flux density q_s (m s^{-1}) and duration t_s (s), resulting in the initial and boundary conditions of:

$$t \le 0,\ t \ge t_s,\quad q(0,t) = w(0,t) = 0 \tag{16a}$$

$$0 \le t \le t_s,\ q(0,t) = q_s,\quad w(0,t) = w_s = \left(\frac{q_s}{b}\right)^{1/a} \tag{16b}$$

$$0 \le z \le \infty,\quad q(z,0) = w(z,0) = 0 \tag{16c}$$

where the maximum mobile moisture w_s is the difference between maximum soil moisture θ_{max} and final soil moisture θ_{end} (Fig. 1).

The solution for $w(z,t)$, for $z \le z_I$ (where z_I is the depth at which the drainage front intercepts the wetting front) is:

$$w(z,t) = 0 \qquad 0 \le t \le t_W(z) \tag{17a}$$

$$w(z,t) = w_s \qquad t_W(z) \le t \le t_D(z) \tag{17b}$$

$$w(z,t) = w_s \left\{\frac{\left(t_D(z) - t_s\right)}{\left(t - t_s\right)}\right\}^{1/(a-1)} \qquad t \ge t_D(z) \tag{17c}$$

where $t_W(z)$ and $t_D(z)$ are the arrival times of the wetting and drainage fronts at depth z, respectively. Equations (17) indicate that the square pulse infiltrates as a shock wave without being spread. After input has ceased, the water content at the surface drops to 0, and a draining front starts moving. It travels with velocity $c_D = c$, which is greater than c_W. After the draining front intercepts the wetting front, a single-crested function $w(z,t)$ for depths $z \ge z_I$ evolves, and the water content of the peak begins to decrease. For $z \le z_I$ the characteristics of the wetting and draining fronts are straight lines intersecting at (z_I,t_I). The characteristics correspond to the evolution of two shock waves, one originating from the applied water content w_s at time $t = 0$ and the other from the reduction to zero of the water content at the surface when input ceases at time

$t = t_s$. The kinematic wave model applies in two modes, the *w*-mode presented above and the *q*-mode that is obtained by writing equation (17) in terms of q using relationship (12) for times $t \geq t_D(Z)$. The *q*-mode allows for input–output experiments, and is applied here to test the validity of the KWA. Typically, these experiments consist of irrigating on the surface of a soil and measuring the drainage hydrograph at a given depth. The *w*-mode requires rapid measurement of soil moisture at a given depth. Several tests of the accuracy of the approach to predict infiltration and drainage in soil with macropores have been carried out by using either the *w*- or *q*-modes (Mdaghri-Alaoui & Germann, 1998; Mdaghri-Alaoui *et al*., 1997).

The total flow volume, $V(Z)$, which has passed Z as a kinematic wave during $t_W(Z) < t < \infty$ follows from integration of equation (17) under the consideration of equation (12):

$$V(Z) = b\mathrm{w}_s^a \left[\int_{t_W}^{t_D} \mathrm{d}t + (t_D - t_s)^{a/(a-1)} \int_{t_D}^{\infty} (t - t_s)^{-a(a-1)} \mathrm{d}t \right] \tag{18}$$

leading to:

$$V(Z) = b\mathrm{w}_s^a \left[at_D \int_{t_W}^{t_D} \mathrm{d}t - t_W - (a-1)t_s \right] = b\mathrm{w}_s^a(Z)t_s = q_s(Z)t_s \tag{19}$$

The similarity between the MACRO and kinematic wave approaches to macropore flow is evident from comparing equation (4) with equation (12), where the former considers the degree of saturation and the latter the mobile water in the macropores. Indeed, these two equations can be made mathematically equivalent by setting:

$$b = \frac{K_s - K_b}{(\theta_s - \theta_b)^a} \tag{20}$$

Thus, providing that the water exchange with the matrix is negligible (i.e. in the case of a saturated matrix), fitting MACRO and the KWA to measured hydrographs should result in identical values of the exponents n^* and a, while the coefficients should be related through equation (20) by the macroporosity and the kinematic exponent. Since the macropore water content in equation (4) is scaled by the macroporosity $\theta_s - \theta_b$, the conductance parameter, b, in the kinematic wave then takes on a more direct physical meaning in MACRO of the hydraulic conductivity of macropores at full saturation (Šimunek *et al*., in press).

MODEL APPLICATIONS

MACRO model

Initial conditions, boundary conditions and discretization Water balance simulations were run for a period of one day. The soil profile was divided into 15 soil layers. This discretization was defined by the soil properties (i.e. texture). The main interface is at a depth of 0.16 m dividing soil properties in two groups governing the simulated processes. A bottom boundary condition, suitable for lysimeter experiments, was used (i.e. zero water potential but with no inflow of water).

Parameter estimation Saturated hydraulic conductivity K_s, saturated water content θ_s and bulk density were directly measured, while the boundary hydraulic conductivity K_b, boundary water content θ_b, boundary soil water pressure head Ψ_b, pore size distribution index λ, the effective diffusion path length d, and the exponent n^* reflecting pore size distribution were calibrated. The tortuosity factor n was set to 0.5 throughout the soil profile (Mualem, 1976).

Measured parameters The measured saturated water content θ_s was 52% at a depth of 0.12 m and 50% at depths of 0.26 and 0.33 m. For comparison, Table 1 shows the initial and the maximum water content measured with TDR probes. The measured saturated hydraulic conductivity K_s was set to the average value measured in each horizon, i.e. 100 mm h^{-1} between 0 and 0.16 m and 120 mm h^{-1} below 0.16 m depth. The residual water content θ_r was set to zero throughout the soil column (Table 2). Using the program package RETC (Yates *et al*., 1992), the Brooks-Corey equation gave a good fit to the St Peter's Island data, but the parameterization was not considered reliable due in part to the lack of measurements at low pressure head values. The parameters θ_r and λ were therefore adjusted using automatic calibration.

Table 2 Model input parameters: soil hydraulic properties (model calibrated using Run 3).

Depth (cm)	Parameters: θ_s † ($m^3\ m^{-3}$)	θ_b ‡ ($m^3\ m^{-3}$)	θ_r † ($m^3\ m^{-3}$)	ψ_b ‡ (cm)	λ ‡ (-)	K_s † (mm h^{-1})	K_b ‡ (mm h^{-1})	d ‡ (mm)	n^* ‡ (-)
0–8	0.52	0.42	0	30	0.3	100	1	6	4
8–16	0.52	0.42	0	30	0.3	100	1	6	4
16–27	0.50	0.44	0	20	0.1	120	1	12	2
27–31	0.50	0.44	0	20	0.1	120	1	12	2
31–35	0.50	0.44	0	20	0.1	120	1	2	2
35–43	0.50	0.44	0	20	0.1	120	1	2	2

† Measured parameters.
‡ Parameters derived by calibration.
θ_s: saturated water content; θ_b: boundary water content; θ_r: residual water content; ψ_b: boundary tension; λ: pore size distribution index; K_s: saturated water content; K_b: boundary hydraulic conductivity; d: effective diffusion path length; n^*: reflects pore size distribution in the macropores.

Calibration The MACRO model was calibrated for Run 3 (79 mm h^{-1} intensity and 1.14 h duration) using the TDR measurements at three depths: 0.12, 0.26 and 0.33 m. The calibration procedure used a grid-search technique (see for instance Duan *et al*., 1992). The optimal parameter combination was identified by the minimum of the root mean square error, under two constraints: the slope of the regression between predicted and measured values should be in the range 0.9–1.1 and the coefficient of residual mass in the range –0.001 to +0.001. The calibration was carried out using a preliminary version of a software program designed to calibrate the MACRO model (Acutis *et al*., 2001), enabling the automatic execution of the model for each point of the chosen grid and the evaluation of several objective functions under user-defined constraints. Having calibrated the model on Run 3, the model was then tested against the five remaining infiltration runs keeping the same parameter settings.

Parameterization of bromide breakthrough experiment Steady-state water outflow was attained during the infiltration of 80.5 mm bromide solution which lasted 1 h. The input bromide concentration C_0 was 80 mg l^{-1}. Initial water contents at depths of 0.12, 0.26 and 0.33 m were 0.37, 0.275 and 0.27 $m^3 m^{-3}$, respectively. In comparison with the other infiltration experiments, the initial water content at a depth of 0.33 m was the smallest. Solute transport parameters in the model were fixed at known or default values since they have only a small effect on leaching loss. Thus, the diffusion coefficient for Br^- was set to 1.8×10^{-9} m^2 s^{-1}, the dispersivity D_v was set to 0.01 m, and the impedance factor f to 0.5.

Kinematic wave

The exponent a was estimated through a nonlinear curve fitting procedure, applying equation (17c) to the data points of the falling limb of the drainage hydrograph, $t > t_D$. The method of least-squares fitting was applied to the log form of equation (17c). For details see Germann *et al*. (1997).

RESULTS AND DISCUSSION

Model performance

To evaluate model performance, the widely used goodness-of-fit measure based on the error variance, called modelling efficiency E by Nash & Sutcliffe (1970) was used. It has the properties that for a perfect fit, it takes the value 1. For a fit that is no better than assuming that the mean of the data is known, it has the value zero. For models that are worse than this, it takes negative values (Beven, 2001).

MACRO model

Drainage flow Once calibrated for Run 3 (intermediate rainfall intensity), the model also predicted reasonably well the other five runs, using the same parameter set. A fairly good fit of model predictions to the measured seepage was observed (Fig. 2). The discrepancies between observed and simulated outflow increase with decreasing input rate as illustrated by the values of E.

The effective diffusion path length d was varied between 1 and 30 mm in the calibration; a value of 6 mm in the topsoil layer, 12 mm in the middle, and 2 mm in subsoil layer produced the best results. In view of these small values, the simulation results were compared with those obtained from $d = 1$ mm (a nominal value which results in immediate physical equilibrium) throughout the soil profile. No significant differences existed between the various model runs. The small calibrated values of d suggest that the effects of preferential flow were limited during the experiments.

Inspection of soil structure in the field suggested that more pronounced macropore flow through the St Peter's Island soil would be expected. This assumption was not borne out by the results of satisfactory simulations with small values of the effective diffusion path length d. The minor role of existing macropores is most likely due to the sandy texture of the soil. Figure 3 shows the very high water exchange rate *WER*

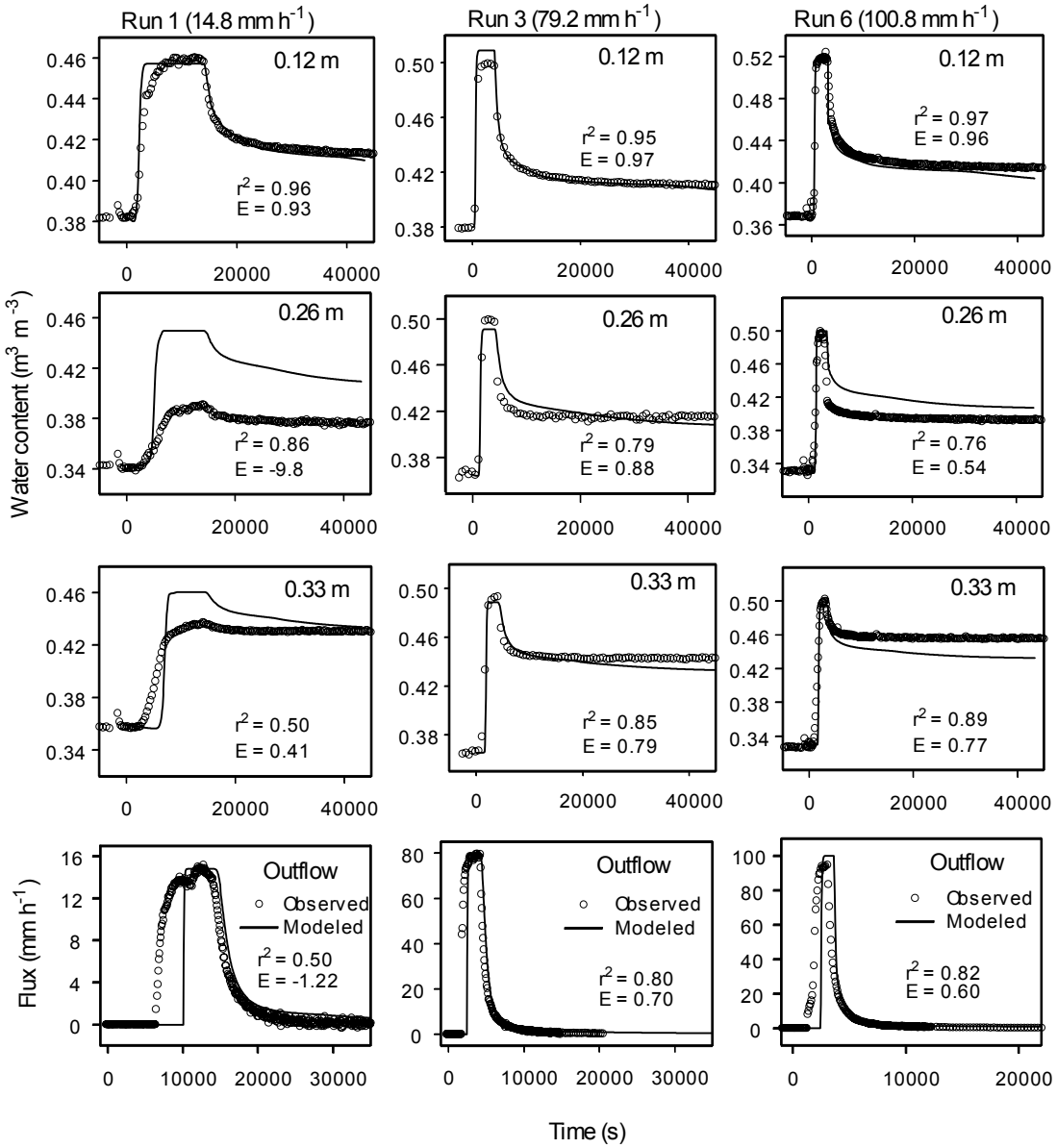

Fig. 2 Measured and modelled water content and water outflow according to the MACRO model for Runs 1, 3 and 6. *E* is the model efficiency by Nash & Sutcliffe, 1970.

(obtained by multiplying S_w by the layer thickness) from macropores to micropores predicted by MACRO. Two significant observations related to this fact are that the predicted *WER* from macropores to micropores increased with increasing input intensity for all runs, and that the *WER* was large in this sandy material, being very close to the input intensity in the sand subsoil.

Water content The model reproduced successfully the pattern of soil moisture measurements at a depth of 0.12 m, where *E* values exceeded 0.9 (Fig. 2). At all depths, the decrease of soil moisture during recession flow was faster with increasing rainfall intensity, and this was also well predicted by the model. However, the *E* values indicate that the agreement between simulated and measured soil water contents was

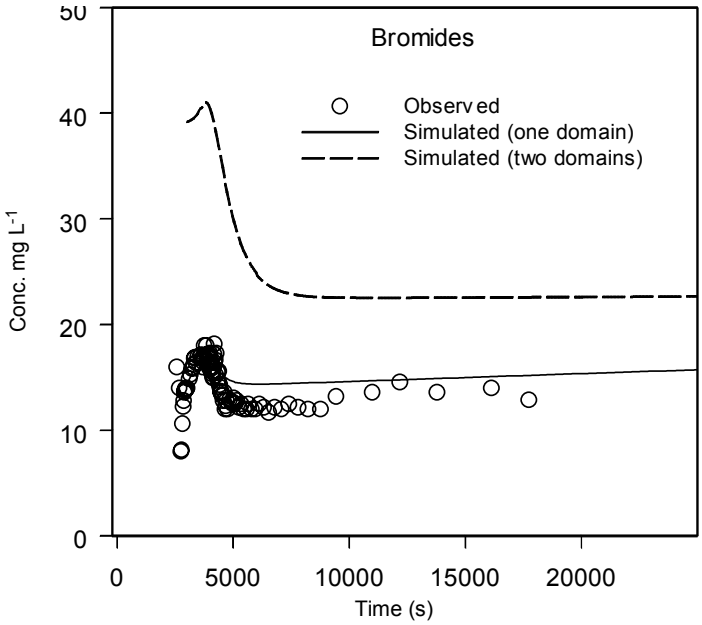

Fig. 4 Measured (o) and predicted (–) bromide concentrations. The solid line refers to the equilibrium conditions and the broken line refers to the non-equilibrium conditions.

the high dilution due to the mixing with "old" water stored in micropores. The model predictions of bromide transport with and without physical non-equilibrium are shown in Fig. 4. As with the water flows, the best simulation was obtained with small values of d reflecting equilibrium between flow domains, while larger d values overestimated bromide concentration in the outflow.

Kinematic wave approach (KWA)

Drainage flow The parameter a obtained from the analysis of outflow q according to the KWA indicates the type of flow near the bottom of the column, whereas when it is calculated from an analysis of soil moisture, it reveals the type of flow at the depth of θ measurement. The exponent a varied within the narrow range of $4 \leq a \leq 5.6$ (Table 3), indicating intermediate flow according to Germann & Di Pietro (1996), who classified flow in soils as being dominated by momentum dissipation (i.e. macropore flow) when $2.0 \leq a \leq 3.0$, by the diffusion of capillary potential (i.e. matrix flow) when $a \geq \approx 8$, and showing intermediate behaviour when $3.0 \leq a \leq 8.0$.

For the low and high intensities (Runs 1 and 6), a exceeded 5. At higher intensities, more pores may contribute to the flux and its spatial distribution may be relatively more homogeneous. At intermediate rates, only some of the coarser pores contribute to the total water flux.

Water content The variation of soil moisture at depths of 0.26 and 0.33 m during Run 1 shows a monotonous increase of soil moisture without a rapid decrease shortly after the cessation of infiltration (Fig. 5). This type of reaction indicates a diffusive process which is dominated by capillarity. Consequently, it was not analysed according to the KWA (Table 3). An example of observed and modelled soil moisture

Table 3 Calculated values of exponent a from the volume flux density $q(Z,t)$ and soil moisture $w(z,t)$ and calculated volume of water flowing through macropores according to the KWA for the six infiltration runs.

Run	1	2	3	4	5	6
Calculated values of exponent a from the volume flux density analysis:						
a (-)	5.42	4.06	4.77	4.73	4.38	5.60
r^2	0.95	0.95	0.98	0.96	0.97	0.97
Calculated values of exponent a from the soil moisture analysis:						
Depth 0.12 m:						
a (-)	5.80	5.41	4.35	5.07	5.14	4.50
r^2	0.99	0.98	0.99	0.99	0.99	0.99
Depth 0.26 m:						
a (-)	-	8.06	5.81	9.29	6.94	4.83
r^2	-	0.98	0.98	0.99	0.84	0.89
Depth 0.33 m:						
a (-)	-	19.74	9.60	13.41	15.41	11.36
r^2	-	0.96	0.96	0.97	0.97	0.96
Calculated volume of water flowing through macropores:						
V_0 (infiltrated)	57	106	90.2	103.5	105	84
$V_{0.12}$	67	139	62	64	58	49
$V_{0.12}/V_0$	1.18	1.31	0.69	0.62	0.55	0.58
$V_{0.26}$	-	107	191	420	278	903
$V_{0.26}/V_0$	-	1	2.12	4.06	2.65	10.75
$V_{0.33}$	-	79	120	162	123	66
$V_{0.33}/V_0$	-	0.75	1.33	1.56	1.17	0.79

$V_{0.12}$, $V_{0.26}$ and $V_{0.33}$ are the values of calculated volume in mm at depths of 0.12, 0.26 and 0.33 m, respectively.

$\theta(z,t)$ and the drainage hydrographs are shown in Fig. 5. The observed and calculated parameters resulting from soil moisture simulation at 0.12, 0.26 and 0.33 m are shown in Table 3. The exponent a at 0.12 m varied from 4 to 6. At 0.26 m, it increased slightly and varied between 5 and 9. The a values increased even more at 0.33 m and lay between 10 and 20. This was true for all six infiltration runs. The increase of the exponent a with increasing depth suggests that the wetting front increasingly dispersed as it progressed downward, and drainage was increasingly dominated by flow through a restricting network of micropores. At the soil surface, a few macropores transported water to deeper layers, while the remaining water moved as a dispersed wetting front through the micropores. An intermediate flow indicated by the KWA drainage flow analysis results from this "mixed" or two-domain flow regime.

The analysis of water contents shows that the flow in the topsoil is of "intermediate" type and disperses with depth. The drainage flow analysis shows an "intermediate" flow type when considering the integrated outflow from the column. The results are consistent.

Water balance The volume of water flowing through macropores $V(Z)$ was calculated with equation (19). In seven out of 16 cases, the calculated volume is overestimated, exceeding the irrigation volume input by a factor varying between 2 and 11 (Table 3). For six of these seven cases, $V(Z)$ lies between 1.3 and 4 which is

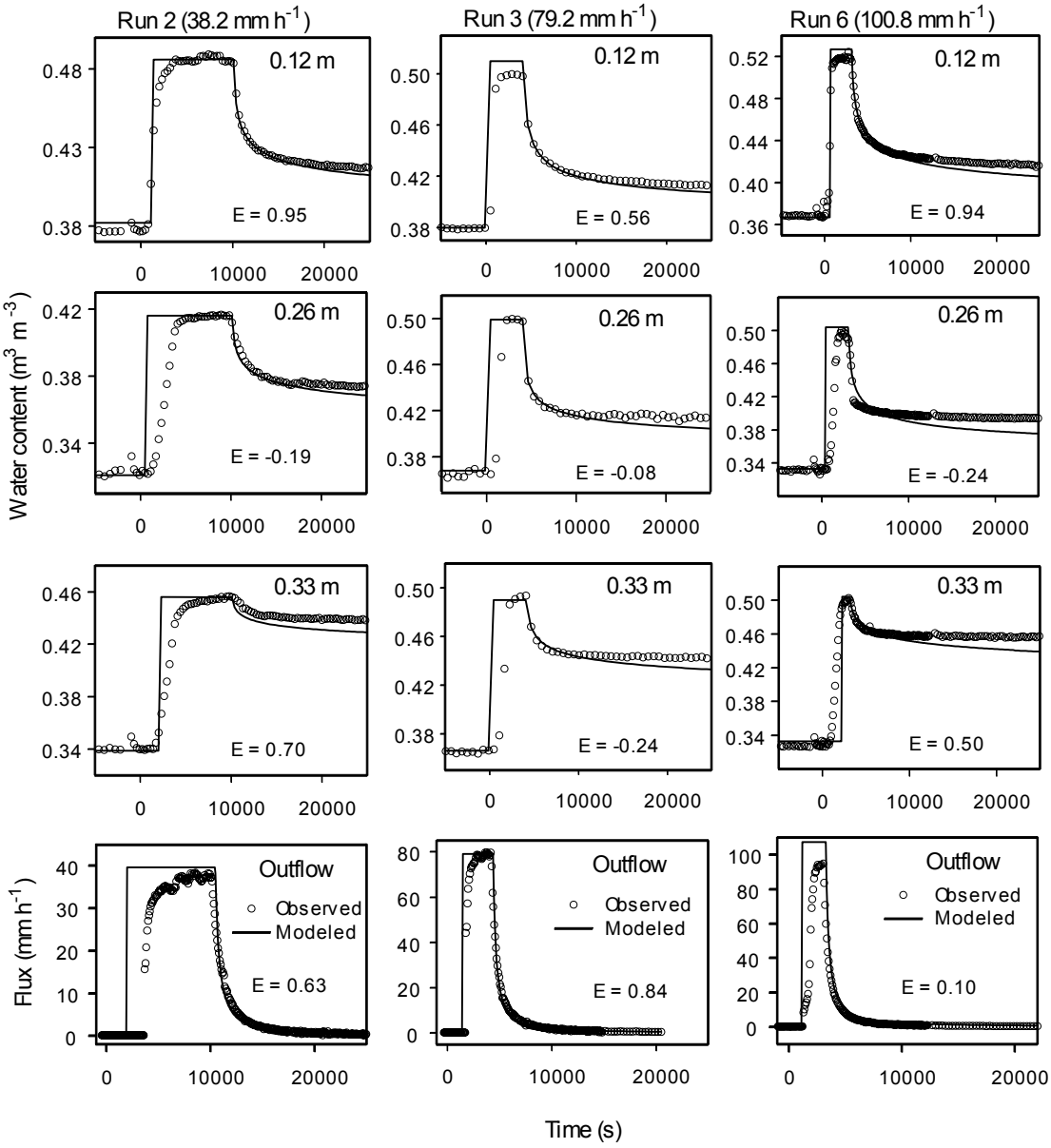

Fig. 5 Measured and modelled water content and water outflow according to the KWA for Runs 2, 3 and 6. *E* is the model efficiency by Nash & Sutcliffe, 1970.

acceptable, and only in one case is it greatly overestimated. These discrepancies can be explained as follows: (a) the dispersion of the wetting front with depth shows that the kinematic wave theory was not applicable at depths of 0.26 and 0.33 m; (b) the estimation of $V(Z)$ depends on the parameter b which is a sensitive parameter in the analysis (Mdaghri-Alaoui, 1998); and (c) the used method of separating the mobile and immobile soil moisture, w and $(\theta - w)$, is promising and does permit the application of kinematic wave theory to describe variations in soil moisture. However, the discrepancies in the water balance suggest that this separation could not always properly account for the losses from macropores to micropores during the wave propagation. An explicit and dynamic treatment of macropore/matrix interactions may be necessary.

Comparison of MACRO and the KWA

The derived parameters of both MACRO and KWA indicated the absence of pure macropore flow. The MACRO model indicated that diffusive matrix flow dominated, based on outflow and water content measurements, and this was confirmed by the consistent validation on the bromide breakthrough data. The KWA indicated an "intermediate" flow type with a significant increase of dispersion with depth. The increase of dispersion with depth indicated by the increase of the exponent a in the KWA is consistent with the high *WER* in the subsoil predicted by MACRO, which was close to the input rate.

The absence of dominant macropore flow in this structured sandy soil as indicated by the two models was in contrast to our expectation because of the abundance of macropores and the high application rates. This unexpected result can be explained by the very efficient lateral mass exchange in the permeable sandy soil. This also shows that, even if macropores are present, they do not necessarily allow non-equilibrium conditions to develop in water pressures or tracer concentrations.

The fitted values of n^* (equation (4)) in MACRO were equal to 4 in the topsoil and 2 in the subsoil, whereas the calculated values of the exponent a (equation (12)) were in the range $4 \leq a \leq 5.6$. The difference between these parameter values (which should be mathematically identical) results from the fact that, while equation (12) describes flow in a single pore domain (mobile water) in the KWA, equation (4) is applied only to the macropore region in MACRO. The larger a values in the KWA are needed to account for the diffusive matrix flow component, which in MACRO is accounted for by Richards' equation.

The boundary water content used for the simulation in MACRO (θ_b) and θ_{end} used in KWA were independently estimated. The value of θ_b was obtained by calibration, while θ_{end} was obtained from observations. The resulting values of θ_b (θ_b at 0.12 m = 42%; θ_b at 0.26 and 0.33 m = 44%) are within the range of the observed values of θ_{end} ($41\% \leq \theta_{end}$ at 0.12 m $\leq 43\%$; $37\% \leq \theta_{end}$ at 0.26 m $\leq 42\%$; $43.7\% \leq \theta_{end}$ at 0.33 m $\leq 45.4\%$), except at 0.26 m where they differ slightly. This encouraging result suggests that the boundary water content θ_b used in MACRO can be directly determined from observations if the water content is measured at different depths. Despite the satisfactory results of the two models, the boundary water content was the most difficult parameter to estimate. Errors in θ_b and θ_{end} can explain the discrepancies between observed and modelled water contents at 0.26 m depth by the MACRO model and the underestimates of the macropore volume at the same depth by the KWA.

CONCLUDING REMARKS

Once calibrated for Run 3 (intermediate intensity), the MACRO model was able to reproduce quite well water flow and bromide breakthrough in the remaining infiltration experiments. The MACRO model run under equilibrium conditions ($d = 1$ mm) described fairly well the soil water movement, and tracer transport in the sandy soil (St Peter's Island) even at high input rates. In general, some discrepancies between model predictions and measurements were noted at a depth of 0.26 m in the column in drier soil with initial water contents less than or equal to 34% by volume (see also Kätterer *et al*., 2001).

The MACRO model requires many soil hydraulic properties, some of which are best derived by automatic calibration. This is time-consuming, and a successful outcome also depends critically on the quality and quantity of the experimental data used for this purpose (Jarvis, 1999).

The KWA has the advantage of simplicity but its application is restricted to determine the type of flow, based on high time resolution measurements of soil moisture and water outflow. The model can be used to analyse preferential flow (Germann & Di Pietro, 1996) as well as intermediate flow regimes (this study) in variably saturated porous media. Measured drainage and soil moisture variations were reasonably well simulated by this approach. The applicability of the model to both drainage outflow and moisture variations suggests that the exponent *a* indicates which flow type dominates: matrix or macropore. The analysis of soil moisture indicated that the exponent *a* increased with increasing depth suggesting an increase of the wetting front dispersion with depth. The simple method used to separate the two types of soil moisture (mobile/immobile) contributing to rapid and diffusive flow respectively is promising, but was not sufficient to reproduce the water balance based on simple measurements of water content by TDR probes. To improve the water balance calculations, further investigations are needed.

In the future, it is necessary to perform these experiments in several different soil types which exhibit pure macropore, intermediate and matrix flow to achieve a greater understanding of flow and transport processes for a large range of soil types.

Acknowledgement This study was supported by the Swiss National Science Foundation, grant no. 21-36281.92.

REFERENCES

Acutis, M., Mdaghri-Alaoui, A., Jarvis, N. & Donatelli, M. (2001) A software for sensitivity analysis, calibration and inversion of MACRO model. In: *Proc. Second Int. Symp. on Modelling Cropping System* (ed. by M. Bindi, M. Donatelli, J. Porter & M. K. van Ittersum) (Florence, Italy, 16–17 July 2001), 207–208. European Society for Agronomy.

Beven, K. (2001) *Rainfall–Runoff Modelling. The Primer*, 217–254. John Wiley & Sons, Chichester, West Sussex, UK.

Beven, K. & Germann, P. (1981) Water flow in soil macropores, II: A combined flow model. *J. Soil Sci*. **32**, 15–29.

Booltink, H. W. G., Hatano, R. & Bouma, J. (1993) Measurements and simulation of bypass flow in a structured clay soil. *J. Hydrol.* **148**, 149–168.

Brooks, R. H. & Corey, A. T. (1964) Hydraulic properties of porous media. Hydrology Paper no. 3, Colorado State University, Fort Collins, Colorado, USA.

Chen, C. & Wagenet, R. J. (1992) Simulation of water and chemicals in macropore soils, I: Representation of the equivalent macropore influence and its effect on soil-water flow. *J. Hydrol*. **130**, 195–126.

Duan, Q., Gupta, V. K. & Sorooshian, S. (1992) Effective and efficient global optimization for conceptual rainfall–runoff models. *Water Resour. Res*. **28**(4), 1015–1031.

Germann, P. F. (1985) Kinematic wave approach to infiltration and drainage into and from soil macropores. *Trans. Am. Soc. Agric. Engng* **28**, 745–749.

Germann, P. (1990) Preferential flow and the generation of runoff. 1. Boundary layer flow theory. *Water Resour. Res*. **26**(12), 3055–3063.

Germann, P. F. & Di Pietro, L. (1996) When is porous media flow preferential? A hydromechanical perspective. *Geoderma* **74**, 1–21.

Germann, P. F. & Di Pietro, L. (1999) Scales and dimensions of momentum dissipation during preferential flow in soils. *Water Resour. Res*. **35**(5), 1443–1454.

Germann, P. F., Di Pietro, L. & Singh, P. (1997) Momentum of flow in soils assessed with TDR-moisture readings. *Geoderma* **80**, 153–168.

Hoogmoed, W. B. & Bouma, J. (1980) A simulation model for predicting infiltration into cracked clay soil. *Soil Sci. Soc. Am. J*. **44**, 458–461.

Jarvis, N. J. (1994) The MACRO model Version 3.1—Technical description and sample simulations. Reports and Dissertations no. 19, Department of Soil Science, Swedish University of Agricultural Sciences, Uppsala, Sweden.

Jarvis, N. J. (1999) Using preferential flow models for management purposes. In: *Proc. Int. Workshop on Modelling of Transport Processes in Soils at Various Scales in Time and Space* (ed. by J. Feyen & K. Wiyo) (Leuven, Belgium, November 1999), 521–535.

Klute, A. & Dirksen, C. (1986) Hydraulic conductivity and diffusivity: laboratory methods. In: *Methods of Soil Analysis* (second edn), Part 1. *Physical and Mineralogical Methods* (ed. by A. Klute), 687–734. Monograph 9, Am. Soc. Agronomy, Madison, USA.

Kätterer, T., Schmied, B., Abbaspour, K. C. & Schulin, R. (2001) Single- and dual-porosity modelling of multiple tracer transport through soil columns: effects of initial moisture and mode of application. *Eur. J. Soil Sci.* **52**, 25–36.

Lighthill, M. J. & Whitham, G. B. (1955) On kinematic waves: I. Flood movement in long rivers. *Proc. Roy. Soc. London Ser. A* **299**, 281–316.

Mdaghri-Alaoui, A. (1998) Transferts d'eau et de substances (bromures, chlorures et bactériophages) dans des milieux non saturés à porosité bimodale: expérimentation et modélisation. PhD Thesis, Soil Science Section, Institute of Geography, University of Berne, Switzerland.

Mdaghri-Alaoui, A. & Germann, P. (1998) Kinematic wave approach to drainage flow and moisture distribution in a structured soil. *Hydrol. Sci. J.* **43**(4), 561–578.

Mdaghri-Alaoui, A., Germann, P., Lichner, L. & Novak, V. (1997) Preferential transport of water and ^{131}iodide in a clay loam assessed with TDR-techniques and boundary-layer flow theory. *Hydrol. Earth Syst. Sci*. **1**(4), 813–822.

Mualem, Y. (1976) A new model for predicting the hydraulic conductivity of unsaturated porous media. *Water Resour. Res*. **12**, 513–522.

Nash, J. E. & Sutcliffe, J. V. (1970) River flow forecasting through conceptual models 1. A discussion of principles. *J. Hydrol*. **10**, 282–290.

Richards, L. A. (1931) Capillary conduction of liquids in porous mediums. *Physics* **1**, 318–333.

Roth, K., Schulin, R., Flühler, H. & Attinger, W. (1990) Calibration of time domain reflectrometry for water content measurement using a composite dielectric approach. *Water Resour. Res*. **26**, 2267–2274.

Šimunek, J., Jarvis, N. J., van Genuchten, M. T. & Gärdenäs, A. (in press) Review and comparison of models for describing nonequilibrium and preferential flow and transport in the vadose zone. *J. Hydrol*.

Valocchi, A. J. (1990) Use of temporal moment analysis to study reactive solute transport in aggregated porous media. *Geoderma* **46**, 233–247.

Van Genuchten, M. T. & Dalton, F. N. (1986) Models for simulating salt movement in aggregated field soils. *Geoderma* **38**, 165–193.

Yates, S. R., van Genuchten, M. T., Warrick, A. W. & Leij, F. J. (1992) Analysis of measured, predicted, and estimated hydraulic conductivity using the RETC computer program. *Soil Sci. Soc. Am. J*. **56**, 347–354.

Received 14 June 2002; accepted 27 January 2003